Supporting Information

Computer-based First-principles Kinetic Monte Carlo Simulation of

Polyethylene Glycol Degradation in Aqueous Phase UV/H$_2$O$_2$ Advanced Oxidation Process

Prepared for Environmental Science and Technology

Xin Guo[1]

Daisuke Minakata[2]

John Crittenden[1*]

1. School of Civil and Environmental Engineering, Georgia Institute of Technology, 828 West Peachtree Street, Atlanta, GA 30332

2. Department of Civil and Environmental Engineering, Michigan Technological University, 1400 Townsend Drive, Houghton, MI, 49931

*Corresponding author phone: 404-894-5676   fax: 404-894-7896

email: john.crittenden@ce.gatech.edu

List of Figures:

List of Tables:

Validation of kinetic Monte Carlo (KMC) solver

To validate the KMC solver, we solved the degradation mechanisms of acetone and trichloroethylene (TCE) in UV/H_2O_2 process by both solving the ordinary differential equation (ODE) and the KMC solver. For each parent compound, we compared the calculated concentration profiles of major species for the ODE solver and the KMC solver. From Figure SI 1 and Figure SI 2, we can find that for both acetone and TCE, the concentration profiles solved by the KMC solver match the concentration profiles solved by the ODE solver very well.

For this validation, the degradation mechanisms of both parent compounds were predicted by the pathway generator and the reaction rate constants were obtained by three ways: (1) directly obtained from literature, (2) estimated based on similar reactions and (3) estimated by group contribution method (GCM).[1] The initial conditions were listed in Table SI 1 and the elementary reactions can be found in Guo *et. al.*[2]
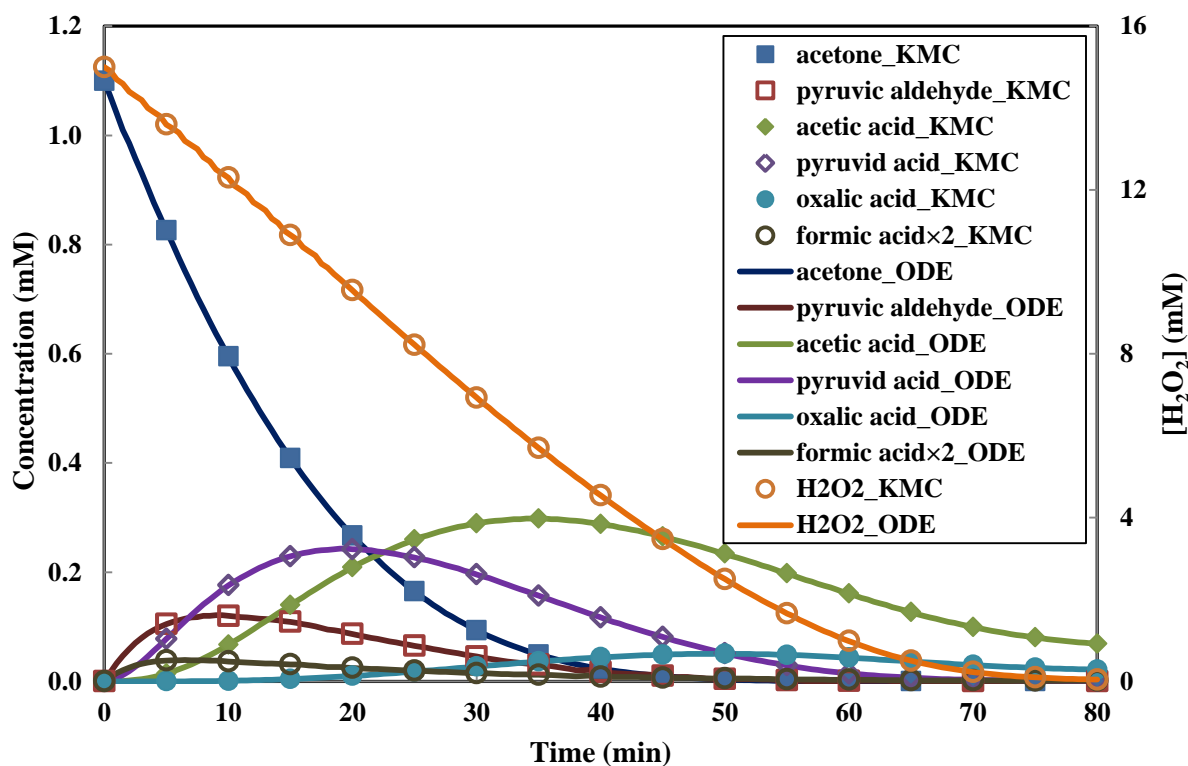
Figure SI 1. Comparison of concentration profiles of major species solved by ODE solver and KMC solver for the degradation of acetone in UV/H_2O_2 process.
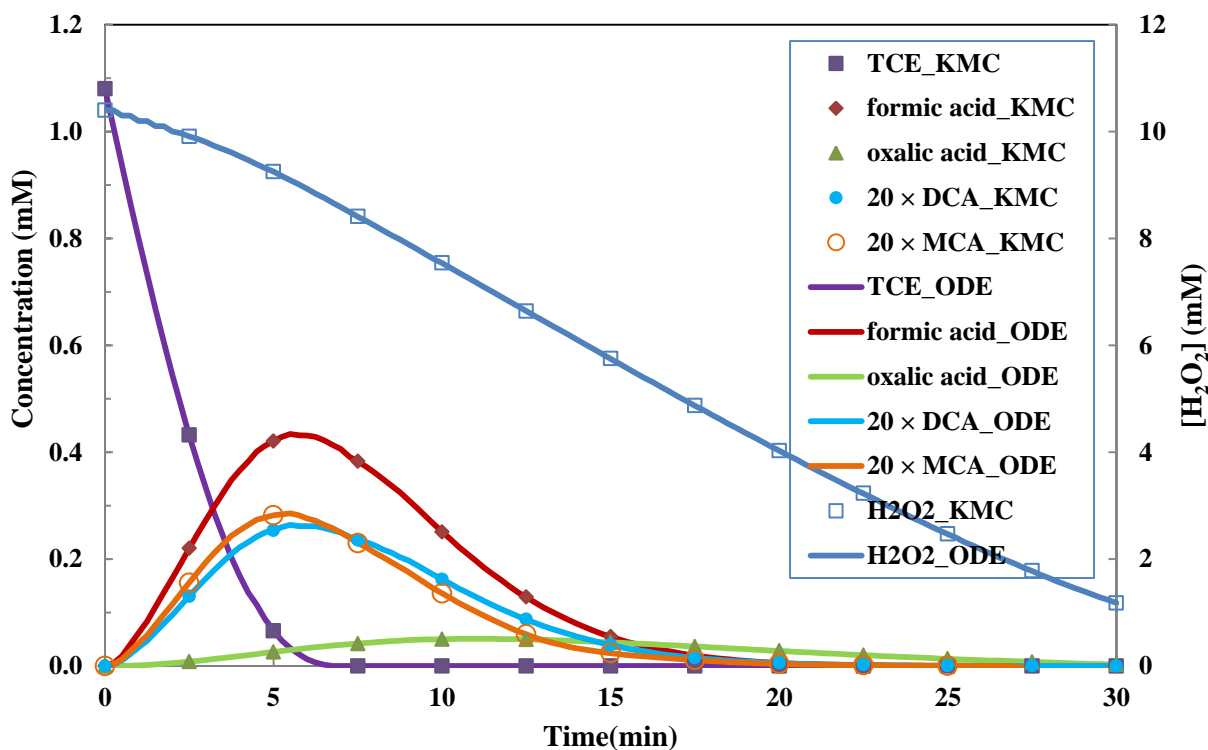
Figure SI 2. Comparison of concentration profiles of major species solved by ODE solver and KMC solver for the degradation of TCE in UV/H_2O_2 process.

Table SI 1. Initial conditions for the simulations of the degradation of acetone and TCE in UV/H_2O_2 process

Parent compound	Acetone	TCE
Initial concentration (mM)	1.1	1.08
Initial concentration of H_2O_2 (mM)	15.0	10.4
Initial pH	5.9	5.9
UV wavelength (nm)	200-300	200-300
UV intensity (Einstein/L•s)	7.79×10^{-6}	7.79×10^{-6}
Reactor type	Completely mixed batch reactor	Completely mixed batch reactor

Reactions included in the degradation mechanism of polyethylene glycol (PEG) in UV/H₂O₂ process generated by the computer-based KMC model

Table SI 2. Reactions included in the generated mechanism for the degradation of PEG in UV/H$_2$O$_2$ process

	Reaction	Rate constant $(M^{-1}s^{-1})$	References
1	$H_2O_2 + hv \rightarrow 2 \bullet OH$	$\Phi_{H2O2} = 0.5$	(3)
2	$H_2O_2 + HO\bullet \rightarrow H_2O + HO_2\bullet$	2.7×10^7	(4)
3	$HO_2^- + HO\bullet \rightarrow OH^- + HO_2\bullet$	7.5×10^9	(4)
4	$H_2O_2 + HO_2\bullet \rightarrow \bullet OH + H_2O + O_2$	3	(4)
5	$H_2O_2 + O_2^-\bullet \rightarrow \bullet OH + OH^- + O_2$	0.13	(4)
6	$2\ HO\bullet \rightarrow H_2O_2$	5.5×10^9	(4)
7	$HO\bullet + HO_2\bullet \rightarrow H_2O + O_2$	6.6×10^9	(5)
8	$2\ HO_2\bullet \rightarrow H_2O_2 + O_2$	8.3×10^5	(6)
9	$O_2^-\bullet + HO_2\bullet \rightarrow HO_2^- + O_2$	9.7×10^7	(6)
10	$HO\bullet + O_2^-\bullet \rightarrow OH^- + O_2$	7×10^9	(5)
11	$-CH_2-CH_2-O-CH_2-CH_2-O- + HO\bullet \rightarrow$ $-CH_2-{}^\bullet CH-O-CH_2-CH_2-O-+H_2O$	6.61×10^8	GCM*
12	$-CH_2-{}^\bullet CH-O-CH_2-CH_2-O- + O_2 \rightarrow$ $-CH_2-CH(OO\bullet)-O-CH_2-CH_2-O-$	1×10^9	Estimated based on (7)
13	$2-CH_2-CH(OO\bullet)-O-CH_2-CH_2-O- \rightarrow$ $2-CH_2-CH(O\bullet)-O-CH_2-CH_2-O- + O_2$	2×10^9	Estimated based on (8)
14	$2-CH_2-CH(OO\bullet)-O-CH_2-CH_2-O- \rightarrow$ $2-CH_2-C(=O)-O-CH_2-CH_2-O- + H_2O_2$	2×10^9	Estimated based on (8)
15	$2-CH_2-CH(OO\bullet)-O-CH_2-CH_2-O- \rightarrow$ $-CH_2-C(=O)-O-CH_2-CH_2-O-+$ $-CH_2-CH(OH)-O-CH_2-CH_2-O-+O_2$	2×10^9	Estimated based on (8)
16	$-CH_2-CH(OH)-O-CH_2-CH_2-O- + O_2 + HO\bullet \rightarrow \rightarrow$ $-CH_2-C(=O)-O-CH_2-CH_2-O- + HO_2\bullet + H_2O$	7.44×10^8	GCM*
17	$-CH_2-CH(O\bullet)-O-CH_2-CH_2-O- \rightarrow$ $-CH_2-CHO + \bullet O-CH_2-CH_2-O-$	$1\times10^5\ s^{-1}$	Estimated based on (9)

18	$-CH_2-CHO+H_2O \xrightarrow{HO\bullet} -CH_2-COOH$	7.81×10^8	GCM*
19	$\bullet O-CH_2-CH_2-O- \rightarrow HCHO + \bullet CH_2-O-$	1×10^5 s^{-1}	Estimated based on (9)
20	$\bullet O-CH_2-CH_2-O-+-CH_2-CH_2-O- \rightarrow$ $HO-CH_2-CH_2-O-+-CH_2-\bullet CH-O-$	1×10^5	Estimated based on (10)
21	$\bullet CH_2-O-+O_2 \rightarrow \bullet OOCH_2-O-$	1×10^9	Estimated based on (7)
22	$2\bullet OOCH_2-O- \rightarrow HOCH_2-O- + OHC-O-+O_2$	2×10^9	Estimated based on (8)
23	$2\bullet OOCH_2-O- \rightarrow 2OHC-O-+H_2O_2$	2×10^9	Estimated based on (8)
24	$2\bullet OOCH_2-O- \rightarrow 2\bullet OCH_2-O-+O_2$	2×10^9	Estimated based on (8)
25	$OHC-O-+H_2O \xrightarrow{HO\bullet} HOOC-O-$	3.66×10^8	GCM*
26	$HOCH_2CH_2OH+HO\bullet \rightarrow HO^\bullet CHCH_2OH+H_2O$	6.93×10^8	GCM*
27	$HO^\bullet CHCH_2OH+O_2 \rightarrow \bullet OOCH(OH)CH_2OH$	1×10^9	Estimated based on (8)
28	$\bullet OOCH(OH)CH_2OH \rightarrow OHCCH_2OH+HO_2\bullet$	1×10^3 s^{-1}	Estimated based on (11)
29	$OHCCH_2OH+H_2O \xrightarrow{HO\bullet} HOOCCH_2OH$	7.81×10^8	GCM*
30	$HOOCCH_2OH+HO\bullet \rightarrow HOOC^\bullet CHOH+H_2O$	6×10^8	(4)
31	$^-OOCCH_2OH+HO\bullet \rightarrow {^-OOC^\bullet}CHOH+H_2O$	8.6×10^8	(4)
32	$HOOC^\bullet CHOH+O_2 \rightarrow \bullet OOCH(OH)COOH$	1×10^9	Estimated based on (8)
33	$\bullet OOCH(OH)COOH \rightarrow OHCCOOH+HO_2\bullet$	1×10^3 s^{-1}	Estimated based on (11)
34	$OHCCOOH+H_2O \xrightarrow{HO\bullet} HOOCCOOH$	2.86×10^7	GCM*
35	$OHCCOOH + H_2O_2 \rightarrow HCOOH + CO_2 + H_2O$	0.3	(12)
36	$HOOCCOOH+{^\bullet}OH \rightarrow CO_2 + CO_2^{\bullet-} + H_2O + H^+$	1.4×10^6	(4)
37	$HOOCCOO^- + {^\bullet}OH \rightarrow CO_2 + CO_2^{\bullet-} + H_2O$	4.7×10^7	(4)
38	$H^+ + OOCCOO^- + {^\bullet}OH \rightarrow CO_2 + CO_2^{\bullet-} + H_2O$	7.7×10^6	(4)
39	$HCHO + H_2O \xrightarrow{HO\bullet} HCOOH$	3.41×10^8	GCM*
40	$HCOOH + {^\bullet}OH \rightarrow CO_2^{\bullet-} + H_2O + H^+$	1.3×10^8	(4)
41	$HCOO^- + {^\bullet}OH \rightarrow CO_2^{\bullet-} + H_2O$	3.2×10^9	(4)
42	$CO_2^{\bullet-} + O_2 \rightarrow CO_2 + O_2^{\bullet-}$	2×10^9	(11)
43	$CO_2^{\bullet-} + H_2O_2 \rightarrow CO_2 + OH^- + {^\bullet}OH$	6.3×10^5	(13)

44	$H_2O_2 \Leftrightarrow H^+ + HO_2^-$	$pK_a = 11.6$	(14)
45	$HO_2\bullet \Leftrightarrow H^+ + O_2^-\bullet$	$pK_a = 4.8$	(15)
46	$HCOOH \Leftrightarrow H^+ + HCOO^-$	$pK_a = 3.75$	(14)
47	$HOOCCOOH \Leftrightarrow H^+ + HOOCCOO^-$	$pK_a = 1.25$	(14)
48	$HOOCCOO^- \Leftrightarrow H^+ + {}^-OOCCOO^-$	$pK_a = 3.81$	(14)
49	$HOCH_2COOH \Leftrightarrow H^+ + HOCH_2COO^-$	$pK_a = 3.8$	(14)

*GCM: the reaction rate constant is predicted by the Group Contribution Method (GCM) developed by Minakata *et al.*[1]

Calculation of averaged molecular weight

The number averaged molecular weight M_n and weight averaged molecular weight M_w are calculated with the following equations

$$M_n = \frac{\sum_{i=1}^{n} M_i N_i}{\sum_{i=1}^{n} N_i} \qquad M_w = \frac{\sum_{i=1}^{n} M_i^2 N_i}{\sum_{i=1}^{n} M_i N_i}$$

where n is the maximum length of PEG, M_i is the molecular weight of PEG with length i, N_i is the population number of PEG with length i.

Sensitivity analysis of the degradation mechanism of PEG in UV/H2O2 process generated by the computer-based first-principles KMC model

To evaluate the importance of each reaction rate constant to the simulation results of the computer-based first-principles KMC model, we applied the one-at-a-time (OAT) sensitivity analysis to the generated degradation mechanism of PEG in UV/H$_2$O$_2$ process. The OAT sensitivity analysis increased each reaction rate constant by 10% in turn and calculated the sensitivity coefficient (SC) of each reaction by the following equation

$$SC_i = \frac{1}{M+N}\left(\sum_{m=1}^{M} \frac{\left| M_{w,m}^{changed} - M_{w,m}^{original} \right|}{M_{w,m}^{original}} + \sum_{n=1}^{N} \frac{\left| C_n^{changed} - C_n^{original} \right|}{C_n^{original}} \right) \tag{1}$$

Where M is the total number of data points for averaged molecular weight (M_w); N is the total

number of data points for concentrations of low molecular weight products (LMWPs); $M_{w,m}^{original}$ is the M_w

before the rate constant of reaction i is changed; $M_{w,m}^{changed}$ is the M_w after the rate constant of reaction i is

changed; $C_n^{original}$ is the concentration of LMWPs before the rate constant of reaction i is changed;

$C_n^{changed}$ is the concentration of LMWPs after the rate constant of reaction i is changed. A reaction rate

constant with high SC indicates that this reaction rate constant is important to the overall simulation

results.

Table SI 3 shows the sensitivity analysis results for the generated degradation mechanism

of PEG in UV/H$_2$O$_2$ process. From this table, we can find that the reaction rate constants that

have significant impact on the simulation results (i.e. SC > 0.005) are consisted of two reaction

types: (1) hydrogen abstraction reaction by hydroxyl radical and (2) special reactions that

involves the radical reactions between H$_2$O$_2$, HO·, and HO$_2$·/O$_2^-$·. The reaction rate constants of

these two reaction types can either be obtained directly from literature or estimated by the

GCM.[1] Table SI 3 also shows that the reaction rate constants that are estimated based on similar

reactions have minor impacts (i.e. SC < 0.005) on the simulation results.

Table SI 3. Sensitivity analysis for the generated degradation mechanism of PEG in UV/H$_2$O$_2$

process

Rank	Reaction	Sensitivity coefficient	Reaction type**	References
1	$H_2O_2 + h\nu \rightarrow 2 \cdot OH$	0.0745	S	(3)
2	$H_2O_2 + HO\bullet \rightarrow H_2O + HO_2\bullet$	0.0551	S	(4)
3	$-CH_2 - CH_2 - O - CH_2 - CH_2 - O - + HO\bullet \rightarrow$ $-CH_2 - {}^\bullet CH - O - CH_2 - CH_2 - O - + H_2O$	0.0479	HA	GCM*
4	$2\ HO_2\bullet \rightarrow H_2O_2 + O_2$	0.0476	S	(6)
5	$H_2O_2 + O_2^-\bullet \rightarrow \bullet OH + OH^- + O_2$	0.0430	S	(4)
6	$HOCH_2CH_2OH + HO\bullet \rightarrow HO{}^\bullet CHCH_2OH + H_2O$	0.0424	HA	GCM*

7	$2\ HO\bullet \rightarrow H_2O_2$	0.0399	S	(4)
8	$HO\bullet + O_2^-\bullet \rightarrow OH^- + O_2$	0.0389	S	(5)
9	$-CH_2-CHO+H_2O \xrightarrow{\ HO\bullet\ } -CH_2-COOH$	0.0301	HA	GCM*
10	$-CH_2-CH(OH)-O-CH_2-CH_2-O-+O_2+HO\bullet\rightarrow\rightarrow$ $-CH_2-C(=O)-O-CH_2-CH_2-O-\ +\ HO_2\bullet\ +\ H_2O$	0.0290	HA	GCM*
11	$OHCCH_2OH+H_2O \xrightarrow{\ HO\bullet\ } HOOCCH_2OH$	0.0283	HA	GCM*
12	$H_2O_2+HO_2\bullet\rightarrow\bullet OH+H_2O+O_2$	0.0276	S	(4)
13	$HO\bullet + HO_2\bullet \rightarrow H_2O+O_2$	0.0252	S	(5)
14	$OHCCOOH+H_2O \xrightarrow{\ HO\bullet\ } HOOCCOOH$	0.0178	HA	GCM*
15	$OHCCOOH+H_2O_2 \rightarrow HCOOH+CO_2+H_2O$	0.0175	S	(12)
16	$O_2^-\bullet + HO_2\bullet \rightarrow HO_2^- + O_2$	0.0165	S	(6)
17	$H^+ + OOCCOO^- + {}^\bullet OH \rightarrow CO_2+CO_2^{\bullet-}+H_2O$	0.0098	HA	(4)
18	$HOOCCOO^- + {}^\bullet OH \rightarrow CO_2+CO_2^{\bullet-}+H_2O$	0.0094	HA	(4)
19	$HOOCCOOH + {}^\bullet OH \rightarrow CO_2+CO_2^{\bullet-}+H_2O+H^+$	0.0090	HA	(4)
20	$HCHO+H_2O \xrightarrow{\ HO\bullet\ } HCOOH$	0.0085	HA	GCM*
21	$HCOO^- + {}^\bullet OH \rightarrow CO_2^{\bullet-}+H_2O$	0.0073	HA	(4)
22	$HCOOH + {}^\bullet OH \rightarrow CO_2^{\bullet-}+H_2O+H^+$	0.0071	HA	(4)
23	$HO_2^- + HO\bullet \rightarrow OH^- + HO_2\bullet$	0.0054	S	(4)
24	$OHC-O-+H_2O \xrightarrow{\ HO\bullet\ } HOOC-O-$	0.0043	HA	GCM*
25	$^-OOCCH_2OH+HO\bullet\rightarrow {}^-OOC{}^\bullet CHOH+H_2O$	0.0023	HA	(4)
26	$HOOCCH_2OH+HO\bullet\rightarrow HOOC{}^\bullet CHOH+H_2O$	0.0021	HA	(4)
27	$2-CH_2-CH(OO\bullet)-O-CH_2-CH_2-O-\ \rightarrow$ $2-CH_2-CH(O\bullet)-O-CH_2-CH_2-O-+O_2$	0.0016	PB	Estimated based on (8)
28	$2-CH_2-CH(OO\bullet)-O-CH_2-CH_2-O-\ \rightarrow$ $2-CH_2-C(=O)-O-CH_2-CH_2-O-\ +\ H_2O_2$	0.0016	PB	Estimated based on (8)
29	$2-CH_2-CH(OO\bullet)-O-CH_2-CH_2-O-\ \rightarrow$ $-CH_2-C(=O)-O-CH_2-CH_2-O-+$ $-CH_2-CH(OH)-O-CH_2-CH_2-O-+O_2$	0.0016	PB	Estimated based on (8)
30	$2\bullet OOCH_2-O-\rightarrow 2\bullet OCH_2-O-+O_2$	0.0008	PB	Estimated based on (8)
31	$2\bullet OOCH_2-O-\rightarrow 2OHC-O-+H_2O_2$	0.0008	PB	Estimated based on (8)
32	$2\bullet OOCH_2-O-\rightarrow HOCH_2-O-\ +\ OHC-O-+O_2$	0.0008	PB	Estimated based on (8)
33	$CO_2^{\bullet-}+O_2\rightarrow CO_2+O_2^{\bullet-}$	0.0003	S	(11)

34	$CO_2^{\bullet-} + H_2O_2 \rightarrow CO_2 + OH^- + {}^\bullet OH$	0.0002	S	(13)
35	$-CH_2 - {}^\bullet CH - O - CH_2 - CH_2 - O - + O_2 \rightarrow$ $-CH_2 - CH(OO\bullet) - O - CH_2 - CH_2 - O -$	1.1E-04	OA	Estimated based on (7)
36	$HOOC^\bullet CHOH + O_2 \rightarrow \bullet OOCH(OH)COOH$	9.2E-05	OA	Estimated based on (7)
37	$-CH_2 - CH(O\bullet) - O - CH_2 - CH_2 - O - \rightarrow$ $-CH_2 - CHO + \bullet O - CH_2 - CH_2 - O -$	8.8E-05	BS	Estimated based on (9)
38	$HO^\bullet CHCH_2OH + O_2 \rightarrow \bullet OOCH(OH)CH_2OH$	8.5E-05	OA	Estimated based on (7)
39	$\bullet OOCH(OH)CH_2OH \rightarrow OHCCH_2OH + HO_2\bullet$	8.4E-05	PH	Estimated based on (11)
40	$\bullet OOCH(OH)COOH \rightarrow OHCCOOH + HO_2\bullet$	6.6E-05	PH	Estimated based on (11)
41	$\bullet O - CH_2 - CH_2 - O - + - CH_2 - CH_2 - O - \rightarrow$ $HO - CH_2 - CH_2 - O - + - CH_2 - {}^\bullet CH - O -$	6.1E-05	HA	Estimated based on (10)
42	$\bullet O - CH_2 - CH_2 - O - \rightarrow HCHO + \bullet CH_2 - O -$	4.3E-06	BS	Estimated based on (9)
43	$\bullet CH_2 - O - + O_2 \rightarrow \bullet OOCH_2 - O -$	3.9E-06	OA	Estimated based on (7)

*GCM: the reaction rate constant is predicted by the Group Contribution Method (GCM)

developed by Minakata *et al*.[1]

**Reaction type:

S: special reaction;

HA: hydrogen abstraction reaction by hydroxyl radical;

PB: bimolecular decay of peroxy radical;

OA: oxygen addition;

BS: β scission;

PH: $HO_2\bullet$ elimination;

      Because the OAT sensitivity analysis is a local sensitivity analysis that requires baseline

values for all reaction rate constants before the analysis and can only reflect the importance of

each reaction rate constant in a small range around the baseline value, these baseline values may have impact on the sensitivity analysis results. As a consequence, we applied multiple times of OAT sensitivity analysis under various baseline values of reaction rate constant of each type of reaction. These varied baseline values cover the possible range of each type of reaction rate constant as shown in Table SI 4. We found that the sensitivity analysis results are same for various baseline values of reaction rate constants within the possible ranges.

Table SI 4. Possible ranges of different types of reaction rate constants in AOPs process

Reaction type	Possible range of reaction rate constant	Reference
H-abstraction reaction by hydroxyl radical	10^7 $M^{-1}s^{-1}$ to 10^9 $M^{-1}s^{-1}$	(4)
Oxygen addition to carbon-centered radical	10^8 $M^{-1}s^{-1}$ to 10^{10} $M^{-1}s^{-1}$	(7)
Bimolecular decay of peroxyl radical	10^8 $M^{-1}s^{-1}$ to 10^9 $M^{-1}s^{-1}$ for primary and secondary preroxyl radical; 10^4 $M^{-1}s^{-1}$ to 10^5 $M^{-1}s^{-1}$ for tertiary preroxyl radical	(11)
$HO_2\bullet$ elimination reaction	10 s^{-1} to 10^5 s^{-1}	(11)
β scission reaction	10^4 s^{-1} to 10^7 s^{-1}	(9)

Detailed information about the implementation of the computer-based first-principles KMC model

The data structure that was used in our CF-KMC model to represent one polymer molecule is shown in Figure SI 3.
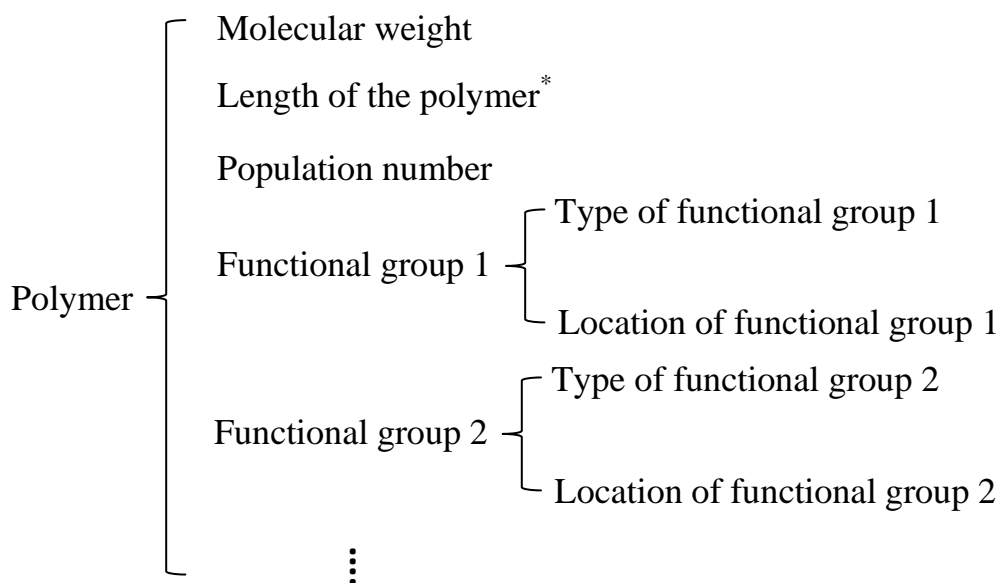
Figure SI 3. Data structure to represent polymer molecules in the CF-KMC model.

*Length of the polymer means the number of repeated monomer units that are contained in the polymer.

From the above figure, we can see that for each polymer, we store the information about molecular weight, length, population number, and types and locations of functional groups for this polymer.

The overall simulation process of the PEG degradation using the CF-KMC model is consisted of three stages. The first stage is to generate the complete degradation pathway of the PEG with the pathway generator. The pathway generator is a computer algorithm that can automatically generate the degradation pathway for the aqueous phase AOPs with reaction rules discovered by previous experiments. For the degradation of the PEG, the pathway generator can make a library that contains the generalized reaction rules for the PEG degradation as listed in the Table SI 2. These generalized reaction rules are discovered by previous experiments. For each polymer, the pathway generator automatically identifies the functional groups in this polymer and predicts potential reactions that can occur for these functional groups based on the

generalized reaction rules. These potential reactions are stored in a reaction pool and the information (e.g., length, molecular weight, and types and locations of functional groups) about the products that are produced from these potential reactions is also stored. Then, these products are fed to the pathway generator again as the inputs and new species that can be produced from these products are generated and stored. The above process is performed iteratively until there is no more new species that can be produced. For the degradation of PEG in our study, we totally predicted 522,057 species and 696,183 reactions by the pathway generator. The detailed information about the pathway generator can be found in Li *et. al.*[9]

The following example shows how we use the pathway generator to predict the degradation of a PEG molecule. First, we make the data structure of the PEG molecule as the input to the pathway generator as shown in Figure SI 4. Then, the pathway generator automatically predicts hydrogen-atom abstraction reaction pathway by HO•. As an example, we only show the situation where the 80th carbon of the polymer chain is attacked as an example. At last, the pathway generator store this predicted reaction in the reaction pool and generates the data structure of the product which has the information about the type and location of the produced functional group, inner-carbon-centered radical. This product will be fed to the pathway generator again as the input and new species will be produced. This process will be performed iteratively until no more new species are produced.

PEG	Molecular weight	3520 g/mole
	Length of the polymer	80
	Population number	10^7

↓ Pathway generator

Product	Molecular weight	3551 g/mole
	Length of the polymer	80
	Population number	0
	Type of functional group	Inner-carbon-centered radical
	Location of function group	On 80th carbon

Figure SI 4. Example of how the pathway generator predicts the degradation of a PEG molecule.

The second stage of the overall simulation process is to obtain the reaction rate constants for all reactions (i.e., 696,183 reactions) that are stored in the reaction pool. For hydroxyl radical reactions, we used the Group Contribution Method (GCM) to predict the reaction rate constants. For other reactions, the rate constants are either obtained from literature or estimated based on similar reactions. The detailed information about how the GCM estimates reaction rate constants can be found in Minakata *et. al.*[1]

The third stage of the overall simulation process is to run the KMC solver to solve the generated degradation mechanism of PEG. As stated in the manuscript, at each time point, the KMC solver selects one reaction to occur from the reaction pool and updates the population

numbers that are stored in the data structures of the reactants and products in this selected reaction. The detailed description about the KMC solver has been stated in the manuscript.

Concentration profiles of low molecular weight products (LMWPs) for the degradation of triethylene glycol (3EG) in UV/H₂O₂ process

In this section, we simulated the degradation of triethylene glycol (3EG) in UV/H_2O_2 process with the computer-aided KMC model and calculated the concentration profiles of 3EG and LMWPs (i.e. diethylene glycol (2EG), ethylene glycol (EG), and formic acid). We compared these calculated concentration profiles with experimental data reported by Santos *et al.*[16] Figure SI 5 shows that the calculated concentration profiles are in a good agreement with the experimental data. It should be noted that since Santos *et al.*[16] only reported time-dependent profiles of peak height for the high performance liquid chromatography (HPLC) for each species, we used these peak heights to represent the relative concentrations of each species in this case.

The degradation pathway of 3EG was generated by the pathway generator as shown in Figure SI 6 and the reaction rate constants obtained by three ways: (1) directly obtained from literature, (2) estimated based on similar reactions and (3) GCM.[1] The experimental conditions are described by Santos *et al.*[16] The initial concentration of hydrogen peroxide was 0.15 M. The initial concentration of 3EG was 0.18 mM. The wavelength of UV light was 254 nm and the light intensity was 1.63×10^{-5} Einstein/L·s. The initial pH was 5.9. The reactor type was CMBR.
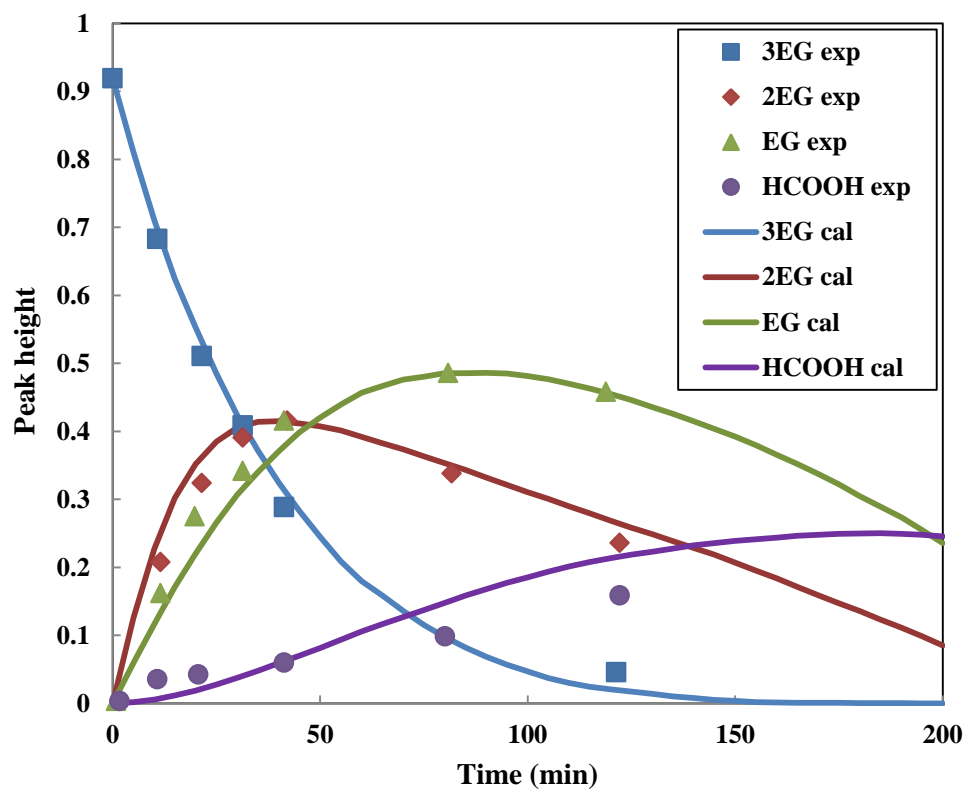
Figure SI 5. Comparison of concentration profiles of 3EG and LMWPs between experimental data[16] and predicted data for the degradation of 3EG during UV/H$_2$O$_2$ process.

HOCH$_2$CH$_2$-O-CH$_2$CH$_2$-O-CH$_2$CH$_2$OH

HO•   HO•   HO•

HO•

HOC•HCH$_2$-O-C$_4$H$_9$O$_2$ HOCH$_2$C•H-O-C$_4$H$_9$O$_2$ OH$_5$C$_2$-O-C•HCH$_2$-O-C$_2$H$_5$O

O$_2$

O$_2$

•OOC(OH)HCH$_2$-O-C$_4$H$_9$O$_2$ HOCH$_2$C(OO•)H-O-C$_4$H$_9$O$_2$

O$_2$

OH$_5$C$_2$-O-C(OO•)HCH$_2$-O-C$_2$H$_5$O

OHCCH$_2$-O-C$_4$H$_9$O$_2$ HOCH$_2$C(OH)H-O-C$_4$H$_9$O$_2$

H$_2$O

HOCH$_2$C(O•)H-O-C$_4$H$_9$O$_2$

HOOCCH$_2$-O-C$_4$H$_9$O$_2$ OH$_5$C$_2$-O-C(OH)HCH$_2$-O-C$_2$H$_5$O

HOCH$_2$C(=O)H-O-C$_4$H$_9$O$_2$

OH$_5$C$_2$-O-C(O•)HCH$_2$-O-C$_2$H$_5$O

OH$_5$C$_2$-O-C(=O)HCH$_2$-O-C$_2$H$_5$O

HOOCCOOH + OHCCOOH + CH$_2$OHCOOH + HCOOH

CO$_2$ + H$_2$O
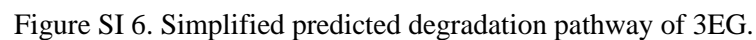
Figure SI 6. Simplified predicted degradation pathway of 3EG.

HOCH$_2$CH$_2$OCH$_2$CH$_2$OH

HO•   HO•

•CH(OH)CH$_2$OCH$_2$CH$_2$OH   HOCH$_2$C•HOCH$_2$CH$_2$OH

↓ O$_2$ ↓ O$_2$

•OOCH(OH)CH$_2$OCH$_2$CH$_2$OH HOCH$_2$CH(OO•)OCH$_2$CH$_2$OH

HOCH$_2$CH(OH)OCH$_2$CH$_2$OH

OHCCH$_2$OCH$_2$CH$_2$OH   HO•

HOCH$_2$CH(O•)OCH$_2$CH$_2$OH

HOOCCH$_2$OCH$_2$CH$_2$OH

HO•   HO• HOCH$_2$CH(=O)OCH$_2$CH$_2$OH

HO•

HOOCC•HOCH$_2$CH$_2$OH HOOCCH$_2$OCH$_2$C•HOH

HOOCCH$_2$OC•HCH$_2$OH

HOOCCOOH + OHCCOOH + CH$_2$OHCOOH + HCOOH

↓

CO$_2$ + H$_2$O
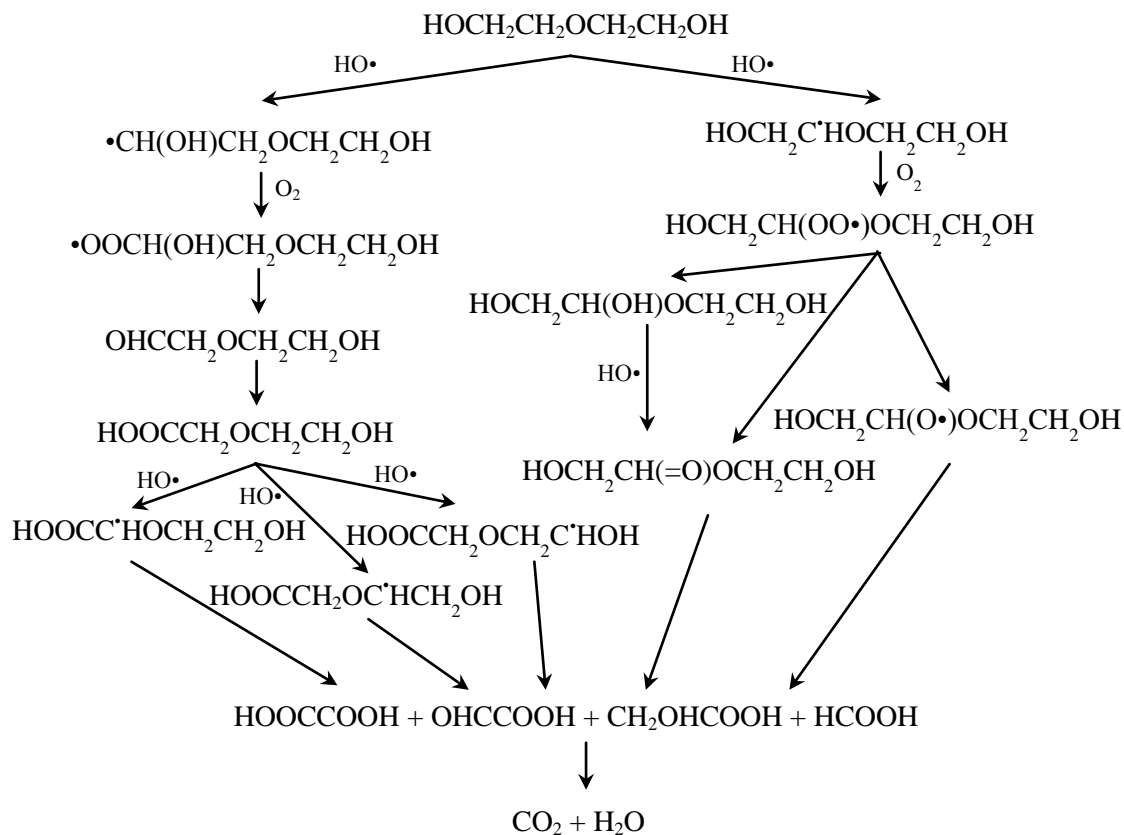
Figure SI 7. Simplified predicted degradation pathway of 2EG.

Prediction of TOC

   Although we do not have the experimental data about the total organic carbon (TOC), we can use our CF-KMC model to predict the change of TOC during the degradation of PEG in the UV/H$_2$O$_2$ process. Figure SI 8 shows that TOC decreases during the degradation of PEG, where TOC$_0$ is the initial TOC. The simulation conditions are the same as stated in the manuscript.
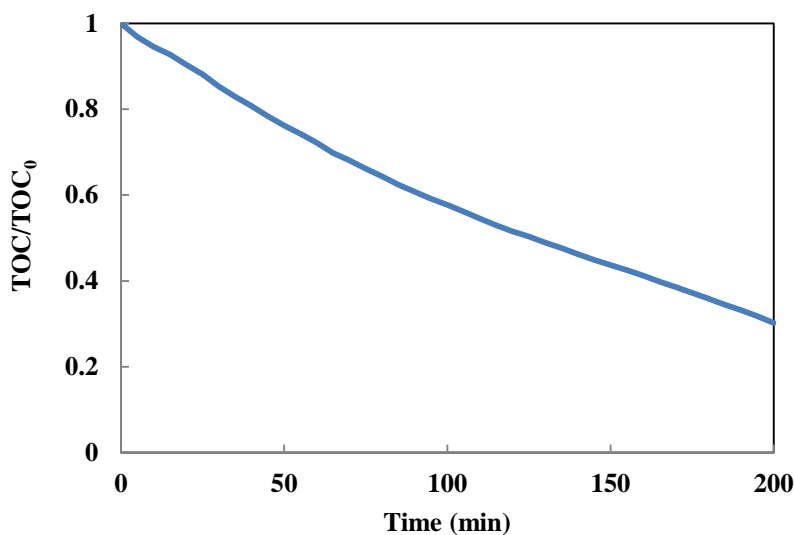
Figure SI 8. Prediction of TOC during the degradation of PEG in UV/H_2O_2 process.

Reference

1. Minakata, D.; Li, K.; Westerhoff, P.; Crittenden, J. Development of a group contribution method to predict aqueous phase hydroxyl radical (HO•) reaction rate constants. *Environ. Sci. Technol*. 2009, 43, 6220-6227.

2. Guo, X.; Minakata, D.; Niu, J.; Crittenden, J. Computer-based first-principles kinetic modeling of degradation pathways and byproduct fates in aqueous-phase advanced oxidation processes. *Environ. Sci. Technol*. 2014, 48, 5718-5725.

3. Hunt, J. P.; Taube, H. The photochemical decomposition of hydrogen peroxide: quantum yields, tracer and fractionation effects. *J. Am. Chem. Soc.* 1952, 74, 5999-6002.

4. Buxton, G.V.; Greenstock, C.L.; Helman, W.P.; Ross, A.B. Critical review of rate constants for reactions of hydrated electrons, hydrogen atoms and hydroxyl radicals (•OH/•O⁻) in aqueous solution. *J. Phys. Chem. Ref. Data*. 1988, 17, 513-886.

5. Elliott, A. J.; Buxton, G. V. Temperature dependence of the reactions hydroxyl-superoxide and hydroxyl-hydroperoxy in water up to 200 °C. *J. Chem. Soc., Faraday Trans.* 1992, 88, 2465-2470.

6. Bielski, H. J.; Benon, H. J.; Cabelli, D. E.; Ravindra, L. A.; Alberta, A. B. Reactivity of perhydroxyl/superoxide radicals in aqueous solution. *J. Phys. Chem. Ref. Data.* 1985, 14, 1041-1100.

7. Neta, P.; Grodkowski, J.; Ross, A.B. Rate constants for reactions of aliphatic carbon-centered radicals in aqueous solution. *J. Phys. Chem. Ref. Data.* 1996, 25, 709-1050.

8. Von Sonntag, C.; Schuchmann, H-P. The elucidation of peroxyl radical reactions in aqueous solution with the help of radiation-chemical methods. *Angew. Chem. Int. Ed. Engl.* 1991, 30, 1229-1253.

9. Li, K.; Crittenden, J. Computerized pathway elucidation for hydroxyl radical-induced chain reaction mechanisms in aqueous phase advanced oxidation processes. *Environ. Sci. Technol.* 2009, 43, 2831-2837.

10. Baignee, A.; Howard, J.A.; Scaiano, J.C.; Stewart, L.C. Absolute rate constants for reactions of cumyloxy in solution. *J. Am. Chem. Soc.* 1983, 105, 6120-6123.

11. Neta, P.; Huie, R.E.; Ross, A.B. Rate constants for reactions of peroxyl radicals in fluid solutions. *J. Phys. Chem. Ref. Data.* 1990, 19, 413-513.

12. Leitzke, A.; Reisz, E.; Flyunt, R.; von Sonntag, C. The reactions of ozone with cinnamic acids: formation and decay of 2-hydroxyperoxy-2-hydroxyacetic acid. *J. Chem. Soc., Perkin Trans.* 2, 2001, 793-797.

13. Schwarz, H. A. Reaction of the hydrated electron with water. *J. Phys. Chem.* 1992, 96, 8937-8941.

14. Perry, R. H.; Green, D. W.; Maloney, J. D. Chemical enginner's handbook 5th edition. McGraw-Hill, New York, 1981.

15. Bielski, H. J.; Benon, H. J.; Cabelli, D. E.; Ravindra, L. A.; Alberta, A. B. Reactivity of perhydroxyl/superoxide radicals in aqueous solution. *J. Phys. Chem. Ref. Data.* 1985, 14, 1041-1100.

16. Santos, L.C.; Poli, A.L.; Cavalheiro, C.C.S.; Neumann, M.G. The UV/H_2O_2 – photodegradation of poly(ethyleneglycol) and model compounds. *J. Braz. Chem. Soc.* 2009, 20, 1467-1472.